Check for updates

Positron Emission Tomographic Measurement of Bone Marrow Blood Flow to the Pelvis and Lumbar Vertebrae in Young Normal Adults

By Daniel Kahn, George J. Weiner, Simona Ben-Haim, Laura L. Boles Ponto, Mark T. Madsen, David L. Bushnell, G. Leonard Watkins, Esther A. Argenyi, and Richard D. Hichwa

Ten young normal adults had pelvic and lumbar vertebral body bone marrow blood flow examined using [^{15}O]water and positron emission tomography (PET) in a study designed to assess the feasibility and reproducibility of the PET technique for measuring marrow blood flow to various marrow regions. The procedure was well tolerated. Repeated blood flow measurements obtained from two consecutive [^{15}O]water exams on each individual subject were highly reproducible. In addition, there was minimal variation in marrow blood flow from individual to individual and no gender differences were noted. In contrast, mean ± SD bone marrow blood flows (expressed as milliliters per minute per 100 g) at selected anatomical sites were significantly different and were as follows: lower lumbar vertebral bodies, 17.6 ± 3.1; most posterior and superior pelvis (conventional site of percutaneous bone marrow biopsy), 14.3 ± 3.1; and total superior pelvis, 11.1 ± 2.0. We conclude that PET is a relatively noninvasive, simple, and reproducible technique for measuring bone marrow blood flow. Marrow blood flow is consistent between normal young subjects, but varies significantly between different anatomic regions of the marrow.

This is a US government work. There are no restrictions on its use.

THE TWO SOURCES OF blood supply of hemopoietically active bone marrow are the nutrient arteries and capillaries from the muscular arteries.[1] The nutrient arteries, the primary source, enter the marrow cavity and ultimately divide into sinusoidal networks. These networks are the principal site of nutrient exchange between the blood and the marrow cells, including both stromal cells and hematopoetic cells.[1-3] The sinusoidal networks or sinuses drain into the central sinus of the marrow cavity. Blood then exits the marrow cavity and enters the venous circulation through emissary veins.[1]

Whereas the vascular anatomy of the bone marrow is well defined, the level of blood flow or perfusion is incompletely understood. The current investigations were designed to determine the blood flow within the pelvic and lumbar spine bone marrow in young normal subjects using positron emission tomography (PET). The results of these studies will be useful in defining normal physiology and as a standard to determine whether blood flow abnormalities are associated with a variety of bone marrow disorders.

MATERIALS AND METHODS

Subject population. Ten normal subjects (5 male and 5 female) volunteered to participate in this prospective study. The average age of the male subjects was 25 years (range, 24 to 26) and of the female subjects was 23 years (range, 20 to 25). The subjects denied having any significant medical problems or abnormalities of their complete blood counts. Apart from 2 of the subjects who were taking oral contraceptives, none of the subjects were taking any medications at the time of the PET examinations. All subjects had normal complete blood counts, which included hemoglobin and hematocrit values, white blood counts with differential values, and platelet counts within 15 days of their PET examination. Before enrollment, each subject signed an informed consent statement that had been approved by the University of Iowa Radiation Protection Committee and the University of Iowa Institutional Review Board for the study of human subjects. All subjects fasted for 4 hours before the PET study.

Imaging technique. The [^{15}O]water procedure for the determination of regional blood flow in units of milliliters per minute per 100 g of tissue was as follows. Under local anesthesia, radial arterial and venous catheters were placed in the nondominant and dominant arms, respectively. The supine subject was positioned "feet-first" (for subject comfort) within the scanner gantry. The laser light guides (indicating slice 1) were aligned using clearly defined palpable pelvic landmarks: the anterior-superior iliac spines and the superior aspects of the posterior iliac crests. This assured that at least the superior half of the pelvis, lower lumbar spine, and the distal aorta were within the field of view. A system of pliable foam supports and an immobilizer/positioner (Calergo; Victoreen, Carle Place, NY) were used to immobilize the subject in the same position during all scan acquisitions. The laser line system was used to detect and subsequently correct subject motion. Transmission images (approximately 30-minute acquisition time with a minimum of 15,000,000 counts) were taken with a [^{68}Ge]germanium pin source for attenuation correction of the emission images. The transmission images appear like coarse computer tomography (CT) scan images. Like conventional CT images, these images represent the tissue densities. Without changing the subject's position within the scanner, emission ([^{15}O]water) images were then acquired. Fifteen simultaneous slices (10 cm axial field of view) were obtained at a resolution of 5.5 mm in three dimensions with the GE-4096 Plus whole-body PET system (GEMS, Milwaukee, WI). [^{15}O]oxygen was produced by irradiation of 1% oxygen in nitrogen with 8.3 MeV deuterons from an on-site MC-17F cyclotron (Scanditronix, Uppsala, Sweden). The production involved continuously sweeping the cyclotron target with gas (1% O_2/N_2). The resulting [^{15}O]oxygen and nitrogen were then piped directly to the imaging suite, where it was combined with hydrogen and converted catalytically (0.5% palladium on ⅛ inch alumina pellets at approximately 100°C) to [^{15}O]-water, which was trapped immediately into sterile saline for injection.

At time = 0 seconds, a bolus injection of 50 to 75 mCi of [^{15}O]-

From the Departments of Radiology and Internal Medicine, University of Iowa College of Medicine, Iowa City, IA.

Submitted April 26, 1993; accepted October 18, 1993.

Supported in part by Biomedical Research Support Grant RR 05372 from the Biomedical Research Support Branch, Division of Research Facilities and Resources, National Institutes of Health (Bethesda, MD).

Address reprint requests to Daniel Kahn, MD, Nuclear Medicine Section (115), Iowa City VAMC, Iowa City, IA 52246-2208.

The publication costs of this article were defrayed in part by page charge payment. This article must therefore be hereby marked "advertisement" *in accordance with 18 U.S.C. section 1734 solely to indicate this fact.*

This is a US government work. There are no restrictions on its use.

0006-4971/94/8304-0030$0.00/0

Downloaded from http://ashpublications.org/blood/article-pdf/83/4/958/613408/958.pdf by guest on 15 July 2024

water in 5 to 7 mL saline was administered through the venous catheter and was immediately followed by a 20-mL saline bolus flush. Arterial blood sampling and imaging began at the time of injection (t = 0) and continued for 360 seconds. Arterial blood sampling consisted of discrete arterial samples drawn at a rate of 0.5 mL every 5 to 6 seconds for 20 samples, then at a rate of 0.5 mL every 10 to 12 seconds for 20 samples. Discrete blood samples were immediately capped and weighed, and the radioactivity was counted in a well counter (Canberra Model 727, Meriden, CT). All blood radioactivity counts were deadtime and decay-corrected. These values were converted from well counts to PET counts based on a previously determined calibration factor.

Emission imaging consisted of the acquisition of either 36 10-second frames or 12 5-second frames followed by 30 10-second frames. To determine the time-course of bolus transit, time-activity curves were generated for regions of interest placed over one or more major vessels (eg, aorta) within the field of view. The frames representing the first 60 seconds immediately post-bolus transit were summed forming a static image. The summed image was reconstructed into 4 mm pixels in a 128 × 128 matrix using a Butterworth filter (order, 6; cut-off frequency, 0.35 Nyquist) on a VAXstation 4000 (Digital Equipment Corporation, Maynard, MA). Using the above described image, blood curve (expressed in PET counts), and an assumed partition coefficient of 0.90, the regional blood flow was calculated on a pixel-by-pixel basis (ie, construction of the parametric image) based on equation 2 presented below. A partition coefficient of 0.9 was chosen because it is consistent with literature values for tissues such as brain, heart, kidneys, and tumor. Significant alterations in the partition coefficient in the range of flows relevant to this study have little effect on overall blood flow determinations calculated from the autoradiographic method.[4]

The reconstruction software incorporates a scatter correction for all images produced on the GE4096 Plus camera and routinely reconstructed. The scatter correction method used was described by Bergstrom et al.[5] No other scatter corrections (specific to bone/soft tissue) were applied.

The above detailed emission imaging procedure was repeated for a second [^{15}O]water injection 15 minutes after the completion of the first [^{15}O]water emission study.

Theory of blood flow measurement. [^{15}O]Water is a diffusible radioactive tracer used to determine regional blood flow. The theory behind this application is based on Kety-Schmidt's single compartment model for diffusible tracers.[6,7] When a single, static image is acquired, the following equation describes the activity in the tissue:[4,8-15]

$$C_t(t) = fC_a(t) \otimes e^{-[(f/p)+\lambda]t} \quad (1)$$

where $C_t(t)$ is the time varying radioactivity concentration (mCi/mL or counts/voxel) in tissue; $C_a(t)$ is the time varying radioactivity concentration (mCi/mL or counts/s/mL) in arterial blood; f is the local mass specific blood flow (eg, mL/min/100 g tissue); p is the tissue-blood partition coefficient for water (a unitless quantity expressed as a ratio of the distributional volumes, eg, mL of blood/mL of specified tissue); λ is the decay constant (defined as the natural log of 2 [ie, ln 2] divided by the $t_{1/2}$ of the nuclide in units appropriate for the equation) for [^{15}O] (ie, 5.66×10^{-3} s^{-1}); and $\otimes$ is the convolution. PET images are not instantaneous count rates (ie, counts acquired over an infinitesimally small period of time), but rather are the counts determined over a finite period of time (eg, seconds). Therefore, the determined count rate values are represented by the integral over the scanning interval (t = T_1 to T_2). If the half life of the tracer is sufficiently long to permit complete equilibrium (ie, the entire distribution volume), the partition coefficient, p, would approach the theoretical value of 1.0. Because the [^{15}O]water does not completely distribute to all available spaces within the short period of image acquisition and within the useful limits of [^{15}O] decay (ie, 1 to 2 half lives = 122 to 244 seconds), a fixed value, less than 1, of the tissue-blood partition coefficient, p, is assumed (such as 0.9, which is the assumed value for brain).[15] Under these conditions, the equation:

$$\int_{T_1}^{T_2} C_t(t)dt = f\int_{T_1}^{T_2} C_a(t) \otimes e^{-[(f/p)+\lambda]t}dt \quad (2)$$

has only one unknown, f, which was estimated by using a look-up table.[15] The left-hand side of equation [2] is the actual PET measurement or image. This image is a compilation of counts originating in all structures simultaneously, because the cellular and capillary sizes (eg, 10 μm) are much smaller than the scanner resolution dimension. Implementation of this approach requires (1) measurement of total [^{15}O]water activity in regions of interest from time = T_1 to T_2; and (2) measurements of total [^{15}O]water activity in arterial blood from time = 0 (ie, injection time) to T (a time greater than T_2).

Image interpretation and analysis. The transmission images and each set of [^{15}O]water parametric images were visually inspected. Regions of interest were referenced to the transmission images and hand-drawn on several portions of the bone marrow cavity in the pelvis and lower lumbar vertebral bodies. Although the resolution of the scanner does not permit perfect separation of the edges of the bone cortex from the marrow, the higher resolution transmission images allowed the region of the bone marrow cavity to be easily identified. Regions of interest were carefully drawn so that they encompassed predominately bone marrow cavity; based on the significantly greater volume of the marrow cavity compared with cortex in these regions, only a minimal inclusion of bone cortex would be expected. The regions of interest from each subject's transmission images were individually transferred to the exactly registered (ie, the transaxial slice at the same anatomic level) [^{15}O]water parametric images (Fig 1). The transaxial slice containing the most posterior and superior region detected on the transmission image was identified as the customary sites for posterior iliac crest biopsies and was used as the reference slice in each subject (Fig 1). Three slices superior to the reference slice and two slices inferior to the reference slice were used to determine the mean right and left superior hemipelvic and the total superior hemipelvic regional blood flow. Vertebral body regions of interest were drawn on any image that clearly demonstrated this tissue.

The mean blood flow values in specific anatomic regions that extended over multiple image slices were determined from an average of the values weighted by the total number of pixels in the regions of interest from each slice. This process was used to determine the regional blood flow to the superior pelvis, to the right and left hemipelvis, to the lumbar vertebral bodies (including L4 and L5 in all subjects, and L2 to 3 when it was in the field of view), and in the most posterior and superior region of the iliac crest corresponding to the site of bone marrow biopsy. Mean value ± standard deviation was determined for each designated region of the bone marrow. The Student's *t*-test was used to determine if differences in blood flow were statistically significant.

RESULTS

Figure 2 depicts arterial blood, bone marrow, and soft tissue time-activity curves derived from one subject. These regions of interest were hand-drawn on the transmission image and transferred to the registered emission scan as described above. The bone marrow regions of interest in Fig 2 were the right and left hemipelvises at the level of lumbar

Downloaded from http://ashpublications.org/blood/article-pdf/83/4/958/613408/958.pdf by guest on 15 July 2024

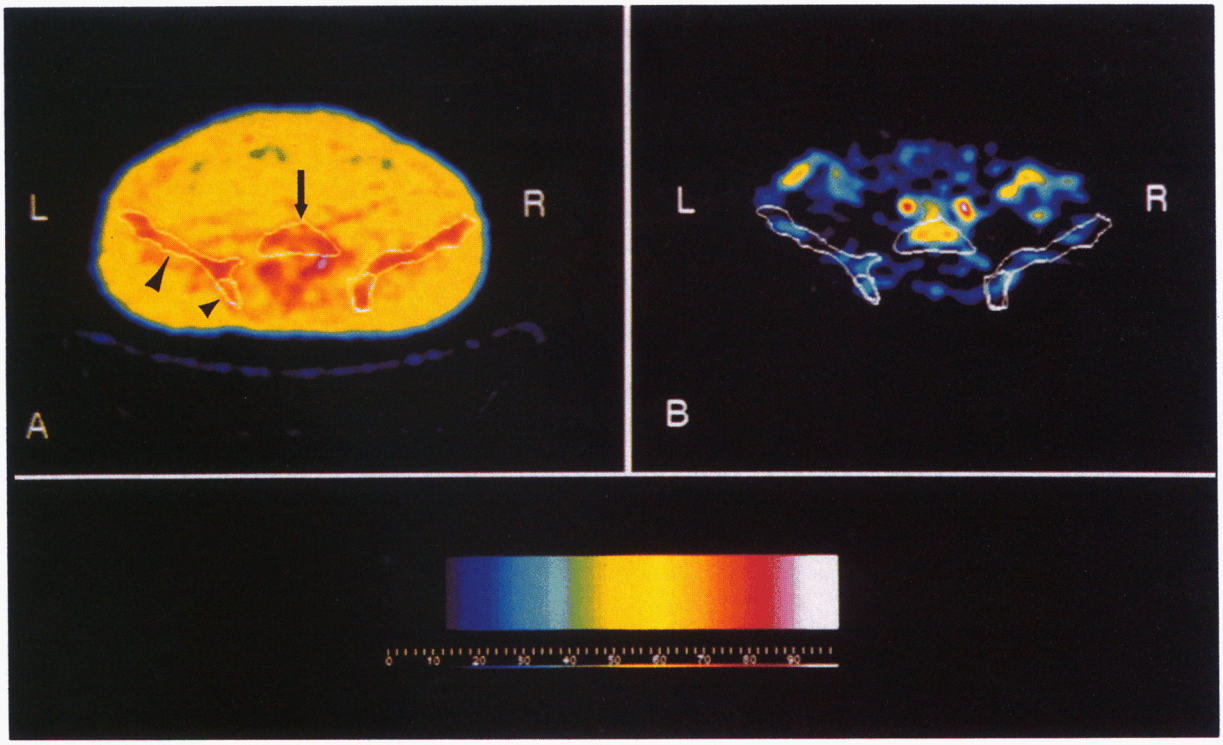

Fig 1. Regions of interest on a single transaxial transmission (A) and [^{15}O]water parametric image (B) in a male subject. The color scale refers to the flow values for the [^{15}O]water image (B) in units of milliliters per minute per 100 g. These images are at the level of the most posterior and superior portions of the iliac wings, the customary site of bone marrow biopsy. The subject is identically positioned relative to the scanner so that the regions of interest drawn around the marrow cavity on the transmission image are directly superimposed onto the [^{15}O]water image to define the activity that represents marrow blood flow. The regions of interest are marked on the left side as follows: entire hemipelvis (large plus small arrowheads), most posterior and superior pelvis (small arrowhead), and vertebral body (arrow). The regions posterior to the vertebral body seen on the transmission scan (in red) likely represent posterior elements; these are not included in the regions of interest. On the [^{15}O]water parametric image, the increased activity seen on the right and left sides anterolaterally probably reflects blood flow to bowel. The two foci of activity seen superior to the vertebral body and off the midline to the right and left represent activity in iliac vessel blood. This was verified by comparing this image to the location of the iliac vessels on the angiographic phase image (not shown) just after the [^{15}O]water injection. The [^{15}O]water activity for the entire pelvis, most posterior and superior pelvis, and vertebral bodies are summed from multiple transaxial slices as described in the Results. The subject is supine, "feet-first" in the scanner gantry. L, left side; R, right side.

vertebra number five. The regions of interest for the soft tissue (right hip and left hip) were oval in shape, chosen lateral to each hemipelvis at the level of lumbar vertebra number five, and principally reflected activity in the gluteal muscle. The right region was 18.1 cm^2 and the left region was 21.3 cm^2 in size. The curves show the distinct difference in blood flow over time between the bone marrow and adjacent soft tissue (gluteal muscle).

The effective spatial resolution of the tomographic slices was approximately 9 mm in three dimensions. The region-of-interest dimensions were all greater than 12 mm. Over the range of time that the blood flow data were collected (as described above in the Materials and Methods) there did not appear to be significant "hot spots" in close proximity to the chosen bone marrow regions of interest. The bone marrow regions of interest were generally distinctly separated from other (typically low count) activity in the image.

Table 1 shows the mean regional bone marrow blood flow in the two sequential PET studies performed on all subjects. There was no statistically significant difference detected in blood flow in each of the regions when comparing the first (PET 1) and second (PET 2) studies. The data from both PET [^{15}O]water examinations were analyzed for males and females (Table 2); no significant difference was detected between these two groups in any of the regions. Table 3 presents the blood flow data derived from both PET [^{15}O]water examinations in all subjects to the pelvis and lumbar vertebral bodies (mean ± SD). The bone marrow blood flow to the most posterior and superior aspect of the pelvis was 14.3 ± 3.1 mL/min/100 g. This blood flow value was significantly higher than the marrow blood flow to the entire superior pelvis, which was 11.1 ± 2.0 mL/min/100 g ($P < .01$). Vertebral body blood flow was 17.6 ± 3.1 mL/min/100 g, and was the highest blood flow detected. It was significantly higher than marrow blood flow to the pelvis ($P < .001$) and to the most posterior and superior aspect of the pelvis ($P < .001$).

DISCUSSION

Recent advances in histologic, immunologic, and genetic techniques have taught us much about the etiology of many

Downloaded from http://ashpublications.org/blood/article-pdf/83/4/958/613408/958.pdf by guest on 15 July 2024

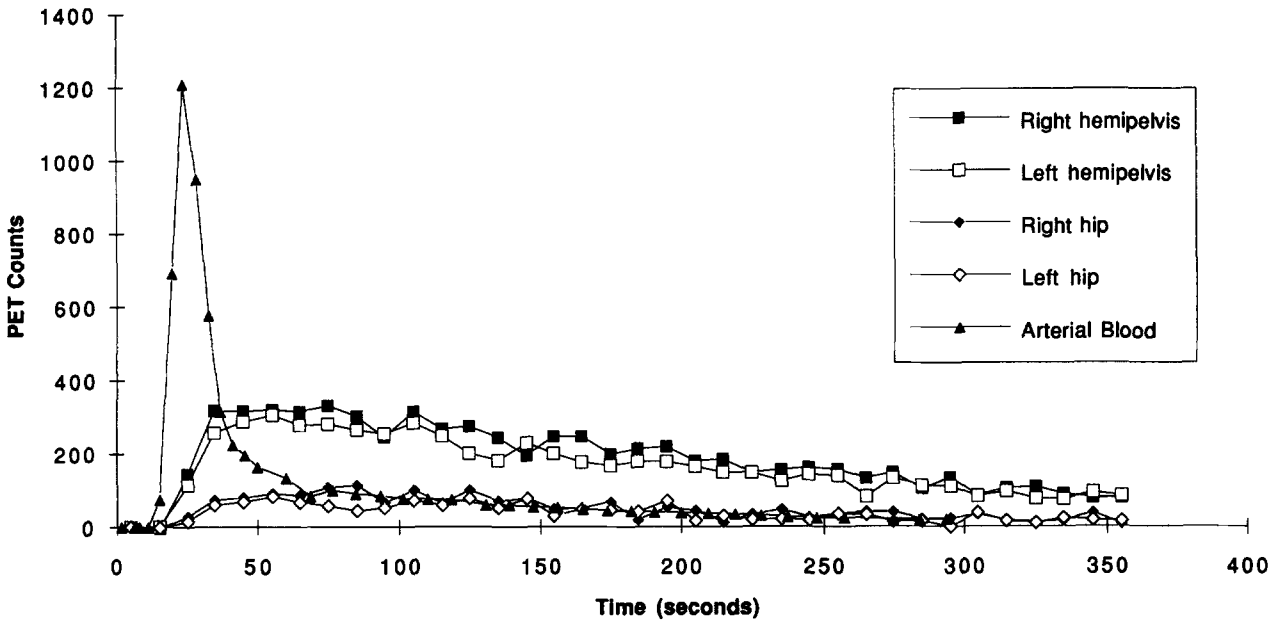

Fig 2. Time-activity curves for arterial blood and from the regions of interest taken from one transaxial slice of the right and left hemipelvises or soft tissue adjacent to the right and left iliac wings (right hip and left hip, respectively). Regions of interest are described in detail in the results.

marrow disorders. Nevertheless, there are a number of marrow abnormalities, including myelofibrosis and many cases of aplastic anemia, that are not well understood. Whereas assays capable of measuring blood flow and perfusion in a variety of nonhematopoetic organs have proven to be invaluable in understanding the pathophysiology and effects of treatment on a broad range of disease states, little is known about marrow blood flow. It is quite possible that physiologic parameters, such as blood flow, which cannot be measured by examination of small random bone marrow samples, could improve our understanding of these disorders. Furthermore, little is known about the impact of therapy on marrow blood flow. The studies described above show that the blood flow to specific portions of the marrow can be measured using PET.

The mean blood flow to the entire pelvis and the most posterior-superior aspect of the pelvis was 11.1 ± 2.0 and 14.3 ± 3.1 mL/min/100 g, respectively. To place this into perspective, Huang et al[13] reported that the regional cerebral blood flow using an [^{15}O]water technique was 59 ± 11 and 20 ± 4 mL/min/100 g (mean ± SD) for gray and white brain matter, respectively. Resting myocardial blood flow in normal volunteers has been reported to be 90 mL/min/100 g by Bergmann et al.[16]

The PET technique described above has the advantage of being relatively noninvasive and offering superior resolution when compared with alternative methods of human bone marrow blood flow measurement. Local marrow blood flow rates in humans have been studied using methods based on clearance rates of [^{131}I]iodine[17] and [^{133}Xe]-xenon.[18] However, the [^{131}I]iodine technique is invasive, and requires an intramedullary injection of the radionuclide. The resolution of the [^{133}Xe]xenon images is distinctly inferior to images produced using PET with [^{15}O]water. For example, it would not be possible to discern smaller regions of interest, such as the most posterior and superior portion

Table 1. Reproducibility of Regional Marrow Blood Flow Measurements (mean ± SD mL/min/100 g) Between Two PET Scans in Same Subject (n = 10)

Region	Flow Values	
	PET 1	PET 2
Left hemipelvis	11.1 ± 2.2	11.1 ± 2.3
Right hemipelvis	11.2 ± 2.0	10.8 ± 1.7
Left postsuperior pelvis	14.6 ± 3.6	14.4 ± 3.5
Right postsuperior pelvis	14.3 ± 2.9	13.8 ± 1.5
Lumbar vertebral bodies	17.6 ± 3.4	17.7 ± 3.1

For region location, see Fig 1. PET 1 and PET 2 refer to two identical [^{15}O] water exams performed 15 minutes apart.

Table 2. Regional Marrow Blood Flow Measurements (mean ± SD mL/min/100 g) in Male and Female Subjects

Region	Flow Values	
	Male (n = 5)	Female (n = 5)
Left hemipelvis	11.1 ± 2.9	11.1 ± 1.3
Right hemipelvis	10.7 ± 2.2	11.3 ± 1.4
Left postsuperior pelvis	14.3 ± 4.2	14.7 ± 2.9
Right postsuperior pelvis	13.8 ± 3.7	14.3 ± 2.0
Lumbar vertebral bodies	17.3 ± 4.1	18.0 ± 2.0

For region location, see Fig 1.

Downloaded from http://ashpublications.org/blood/article-pdf/83/4/958/613408/958.pdf by guest on 15 July 2024

Table 3. Regional Marrow Blood Flow Measurements (mean ± SD mL/min/100 g)

Region	Flow Values
Pelvis	11.1 ± 2.0
Posterior-superior pelvis	14.3 ± 3.1
Vertebral bodies	17.6 ± 3.1

For description of region, see Fig 1.

of the iliac crest, using [^{133}Xe]xenon. Furthermore, [^{133}Xe]-xenon partitions nonuniformly into the tissues that surround bone, meaning that only the more superficial marrow spaces are actually amenable to imaging with this agent. Less superficial marrow spaces (which are surrounded by more soft tissue) such as the vertebral bodies or an entire cross-section of the pelvis are not well imaged with [^{133}Xe]-xenon. Lahtinen et al[18] were able to image a relatively superficial structure such as the greater trochanteric region with [^{133}Xe]xenon; However, PET is able to image the less superficial marrow spaces. The higher resolution of PET permits evaluation of such areas without unacceptable distortion between the region of interest and overlying tissues. PET also has the advantage of using the transmission images (as an attenuation map) to compensate for attenuation of the signal from the marrow by tissues surrounding the bone marrow.

However, because of the finite spatial resolution of any PET system, there is a potential for a partial volume effect. The partial volume effect is negligible when the area of interest is larger than twice the system spatial resolution as specified by the full width at half maximum (FWHM) of the system response function. As the size of the object area decreases past this bound, the measured activity in the region becomes correlated with the activity in the surrounding tissues. This can lead to an artificial variability in the measured blood flow if the regions are on the same order of or smaller than twice the FWHM. Our PET system's FWHM (including the reconstruction filter) was 9 mm. The smallest dimension of the regions used in this study was 12 mm (3 pixels, each 4 mm). For an elongated object of this size and shape, one would obtain an apparent reduction in blood flow of no greater than 15% (resulting from the partial volume effect) if the blood flow in the surrounding tissue were 0.[19] The marrow blood flow values are reported for the entire region of interest and, because the portions of the regions that were 3 pixels represented only a very small fraction of either the right or left hemipelvic regions, we expect that the actual blood flow reduction caused by partial volume effect is less than 15% in these regions. Therefore, although this limitation to PET measurement of pelvic marrow blood flow is real and must be recognized, no corrections were made for the relatively small flow reduction.

In an effort to simplify and make the measurement of marrow blood flow with PET less invasive, we are currently using a technique that eliminates the need for arterial blood sampling. Instead, 3 to 5 samples of peripheral venous blood are used to monitor the blood activity of [^{15}O]water. The [^{15}O] activity levels of these samples are used to derive the activity present in the arterial blood. Avoiding arterial sampling in this manner will allow for the evaluation of a wide spectrum of patients with serious hematologic disorders who otherwise could not be studied because of contraindications to arterial sampling. Quantitative analysis of pelvic bone marrow blood flow in patients with marrow disorders, as determined by [^{15}O]water studies, indicates that changes in blood flow do occur in patients with abnormal bone marrow. For example, the marrows from 3 of 4 patients with acute myelogenous leukemia displayed blood flows that were approximately 2 to 3 times the level seen in normal subjects, but returned to the normal range after chemotherapy (abstract submitted, The American Society of Hematology, 1993). Thus, quantitative determination of blood flow to abnormal bone marrow can be made using PET.

In conclusion, this study demonstrated intrasubject regional blood flow, as measured by PET after the administration of [^{15}O]water, was highly reproducible. Furthermore, measurements were remarkably consistent between young adults, and no significant differences were detected between male or female subjects. However, significant and consistent regional differences in marrow blood flow were noted with the highest blood flow being seen in the vertebral bodies. Blood flow to the region of the iliac crest commonly biopsied (most posterior and superior region on the scan) was modestly though significantly higher than the total pelvic blood flow. Further studies using this technique should allow for the assessment of this as yet minimally explored aspect of human physiology. The ability to measure marrow blood flow reproducibly and accurately will allow for comparison of marrow blood flow to a number of other parameters such as percent marrow cellularity, marrow differential, subject age, the presence of underlying disease, or response to therapies such as hematopoietic growth factors or antileukemic medications.

ACKNOWLEDGMENT

For technical assistance, we gratefully acknowledge the help of Jo Clark, RN, John Richmond, CNMT, and Julie Koeppel, CNMT. For photographic assistance, James E. Olson is also gratefully acknowledged.

REFERENCES

1. Brookes M: The Blood Supply of Bone. London, UK, Butterworths, 1971

2. McCuskey RS, McClugage SG, Younker WJ: Microscopy of living bone marrow in situ. Blood 38:87, 1971

3. McClugage SG, McCuskey RS, Meineke HA: Microscopy of living bone marrow in situ. II. Influence of the microenvironment on hemopoiesis. Blood 38:96, 1971

4. Herscovitch P, Markham J, Raichle ME: Brain blood flow measured with intravenous H_2-^{15}O. I. Theory and error analysis. J Nucl Med 24:782, 1983

5. Bergstrom M, Eriksson L, Bohm C, Blomqvist G, Litton J: Correction for scattered radiation in a ring detector positron camera by integral transformation of the projections. J Comput Assist Tomogr 7:42, 1983

6. Kety S: The theory and application of the exchange of inert gas at the lungs and tissue. Pharmacol Rev 3:1, 1951

Downloaded from http://ashpublications.org/blood/article-pdf/83/4/958/613408/958.pdf by guest on 15 July 2024

7. Schmidt CF: The early days of the indifferent gas method for measuring cerebral blood flow. J Cereb Blood Flow Metab 2:1, 1982

8. Ginsberg MD, Lockwood AH, Busto R, Finn RD, Butler CM, Cendan IE, Goddard J: A simplified *in vivo* autoradiographic strategy for the determination of regional cerebral blood flow by positron emission tomography: Theoretical considerations and validation studies in the rat. J Cereb Blood Flow Metab 2:89, 1982

9. Howard BE, Ginsberg MD, Hassel WR, Lockwood AH, Freed P: On the uniqueness of cerebral blood flow measured by the *in vivo* autoradiographic strategy and positron emission tomography. J Cereb Blood Flow Metab 3:432, 1983

10. Kanno I, Iida H, Miura S, Murakami M, Takahashi K, Sasaki H, Inugami A, Shishido F, Uemura K: A system for cerebral blood flow measurement using an $H_2{}^{15}O$ autoradiographic method and positron emission tomography. J Cereb Blood Flow Metab 7: 143, 1987

11. Raichle ME, Martin WRW, Herscovitch P, Mintun MA, Markham J: Brain blood flow measured with intravenous H_2-^{15}O. II. Implementation and validation. J Nucl Med 24:790, 1983

12. Gambhir SS, Huang SC, Hawkins RA, Phelps ME: A study of the single compartment tracer kinetic model for the measurement of local cerebral blood flow using ^{15}O-water and positron emission tomography. J Cereb Blood Flow Metab 7:13, 1987

13. Huang SC, Carson RE, Hoffman EJ, Carson J, MacDonald N, Barrio JR, Phelps ME: Quantitative measurement of local cerebral blood flow in humans by positron computed tomography and ^{15}O-water. J Cereb Blood Flow Metab 3:141, 1983

14. Koeppe RA, Holden JE, Polcyn RE: Quantitation of local cerebral blood flow and partition coefficient without arterial sampling: Theory and validation. J Cereb Blood Flow Metab 5:214, 1985

15. Koeppe RA, Hutchins GD, Rothley JM, Hichwa RD: Examination of assumptions for local cerebral blood flow studies in PET. J Nucl Med 28:1695, 1987

16. Bergmann SR, Herrero P, Markham J, Weinheimer CJ, Walsh MN: Noninvasive quantitation of myocardial blood flow in human subjects with oxygen-15-labeled water and positron emission tomography. J Am Coll Cardiol 14:639, 1989

17. Petrakis NL, Masouredis SP, Miller P: The local blood flow in human bone marrow in leukemia and neoplastic diseases as determined by the clearance rate of radioiodide ^{131}I. J Clin Invest 32: 952, 1953

18. Lahtinen T, Karjalainen P, Alhava EM: Measurement of bone blood flow with a ^{133}Xe washout method. A preliminary report. Eur J Nucl Med 4:435, 1979

19. Hoffman EJ, Huang SC, Phelps ME: Quantitation in positron emission computed tomography: 1. Effect of object size. J Comput Assist Tomogr 3:299, 1979

20. Weiner GJ, Kahn D, Ponto LLB, Dogan AS, Madsen MT, Bushnell DL, Watkins GL, Argenyi EA, Hichwa RD: Measurement of bone marrow blood flow in patients with acute leukemia and other bone marrow disorders using positron emission tomography. Blood 82:551a, 1992 (abstr)

Downloaded from http://ashpublications.org/blood/article-pdf/83/4/958/613408/958.pdf by guest on 15 July 2024